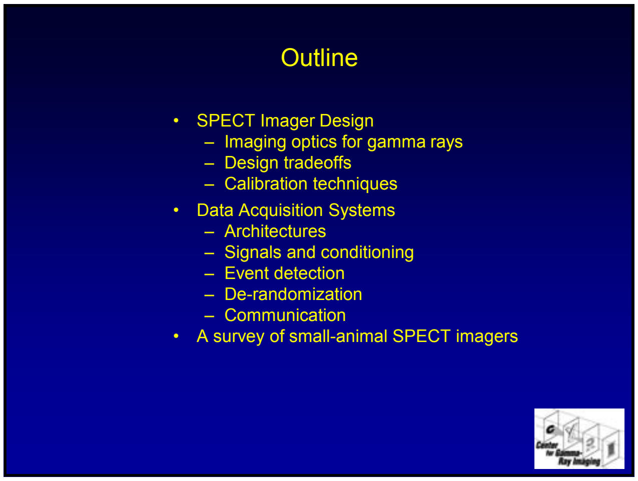

Outline

- SPECT Imager Design
  - Imaging optics for gamma rays
  - Design tradeoffs
  - Calibration techniques
- Data Acquisition Systems
  - Architectures
  - Signals and conditioning
  - Event detection
  - De-randomization
  - Communication
- A survey of small-animal SPECT imagers

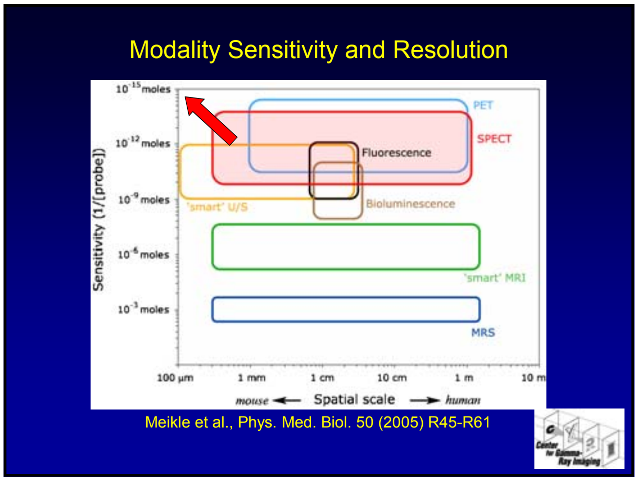

Modality Sensitivity and Resolution

Meikle et al., Phys. Med. Biol. 50 (2005) R45-R61

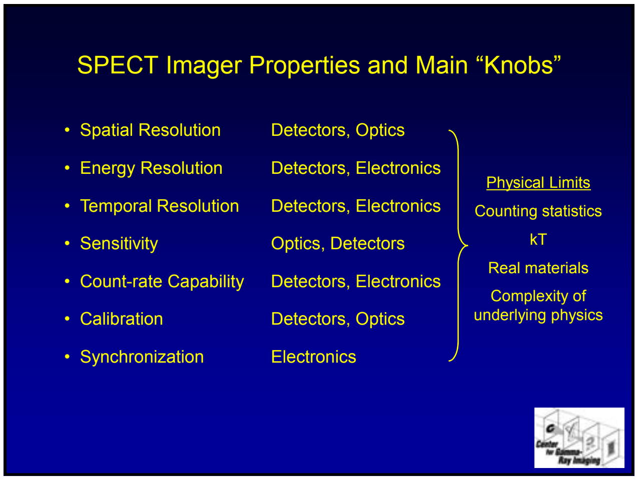

SPECT Imager Properties and Main "Knobs"

• Spatial Resolution	Detectors, Optics	Physical Limits Counting statistics kT Real materials Complexity of underlying physics
• Energy Resolution	Detectors, Electronics	
• Temporal Resolution	Detectors, Electronics	
• Sensitivity	Optics, Detectors	
• Count-rate Capability	Detectors, Electronics	
• Calibration	Detectors, Optics	
• Synchronization	Electronics	

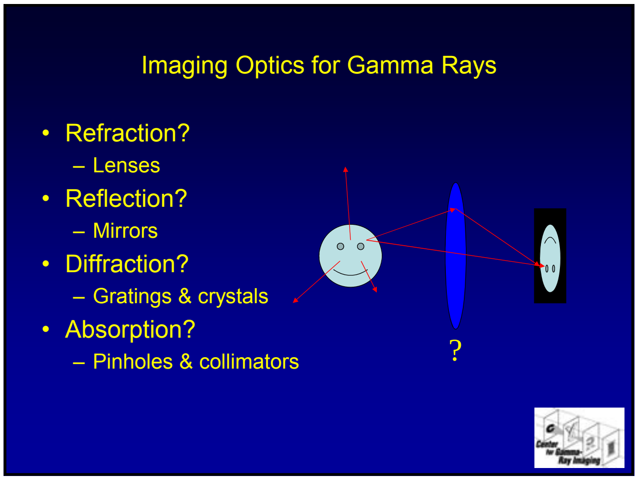

Imaging Optics for Gamma Rays

- Refraction?
  - Lenses
- Reflection?
  - Mirrors
- Diffraction?
  - Gratings & crystals
- Absorption?
  - Pinholes & collimators

Refraction

- The bending of light rays towards the normal in transitions from less to more optically dense media

  $n = 1 - \delta - i\beta$
- Problem is at gamma-ray energies for most materials:

  $\delta \approx 10^{-6}$
- Snell's law:

  $\sin\theta_1 / \sin\theta_2 = n_2/n_1 \approx 1$

  $\theta_1 \approx \theta_2$
- So gamma-ray lenses are physically impossible…

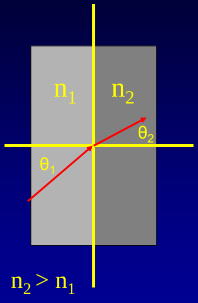

Refraction…

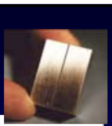

- Or are they?
  - A compound refractive X-ray lens was invented in 1996
    - Practical up to 40 keV
  - But,
    - Long focal lengths (~ 1 m)
    - Small apertures (~ 1 mm)
  - Uses with collimated beams (synchrotrons) and microscopes
  - Another variant is the sawtooth lens:
    - (demo'ed to 80 keV !)

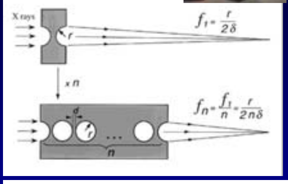

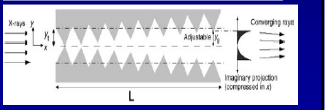

Refraction…

A. Snigirev, V. Kohn, I. Snigireva, B. Lengeler,
"A compound refractive lens for focusing high energy x-rays,"
Nature, 384:49-51, 1996.

B. Lengeler, C. Schroer, J. Tümmler, B. Benner, M. Richwin, A. Snigirev, I. Snigireva, M. Drakopoulos,
"Imaging by parabolic refractive lenses in the hard x-ray range,"
J. Synchrotron Rad., 6: 1153-1167, 1999.

B. Cederström, R. N. Cahn, M. Danielsson, M. Lundqvist, D. R. Nygren,
"Focusing hard x-rays with old LP's,"
Nature, 404: 951, 2000.

Reflection

- The redirection of light rays about the normal at interfaces between media of different *n*
- Occurs when no real solution to Snell's law

  $\sin\theta_2 = (n_1/n_2)\sin\theta_1 \geq 1$

  $\sin\theta_1 \geq n_2/n_1 \approx 1$

  $\sin\theta_1 \approx 90^\circ$
- Problem is at gamma-ray energies for most materials:

  $\Delta\ \delta \approx 10^{-6}$
- So gamma-ray mirrors are physically challenging…

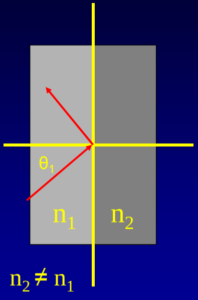

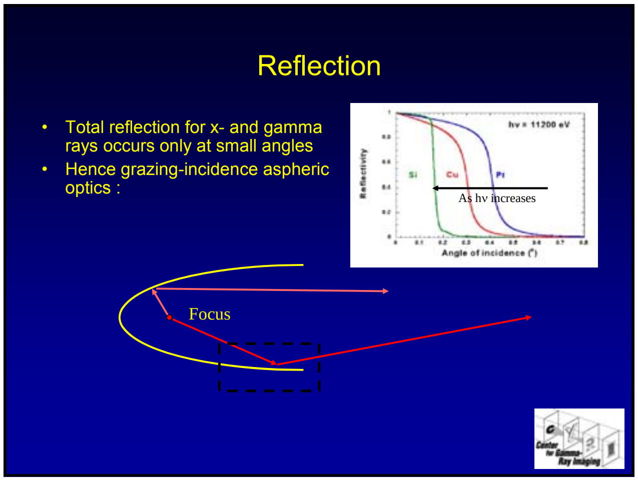

Reflection

- Total reflection for x- and gamma rays occurs only at small angles
- Hence grazing-incidence aspheric optics :

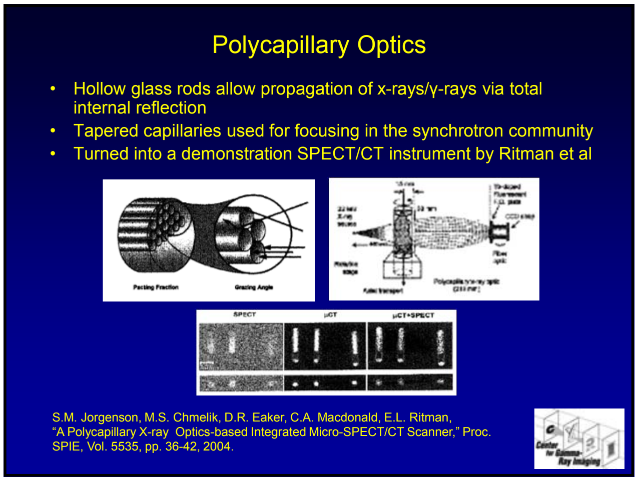

Polycapillary Optics

- Hollow glass rods allow propagation of x-rays/γ-rays via total internal reflection
- Tapered capillaries used for focusing in the synchrotron community
- Turned into a demonstration SPECT/CT instrument by Ritman et al

S.M. Jorgenson, M.S. Chmelik, D.R. Eaker, C.A. Macdonald, E.L. Ritman, "A Polycapillary X-ray Optics-based Integrated Micro-SPECT/CT Scanner," Proc. SPIE, Vol. 5535, pp. 36-42, 2004.

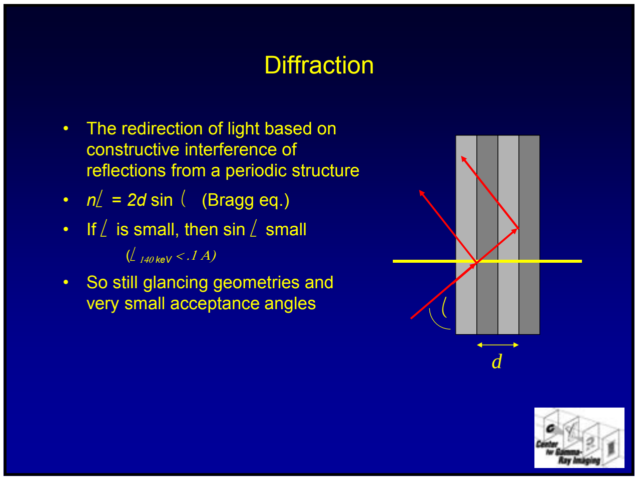

Diffraction

- The redirection of light based on constructive interference of reflections from a periodic structure
- $n\lambda = 2d \sin\theta$ (Bragg eq.)
- If λ is small, then sin λ small

  $(\lambda_{140\,\mathrm{keV}} < .1\ A)$
- So still glancing geometries and very small acceptance angles

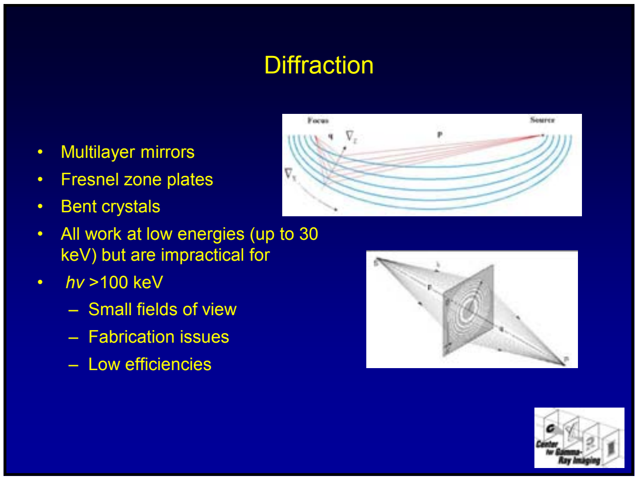

Diffraction

- Multilayer mirrors
- Fresnel zone plates
- Bent crystals
- All work at low energies (up to 30 keV) but are impractical for
- *hv* >100 keV
  - Small fields of view
  - Fabrication issues
  - Low efficiencies

Multilayer Mirror Optics

- A single mirror has low collection efficiency
- NASA has pioneered multi-shell mirrors made up of arrays of metal foils
- Practical up to 35 keV
  - Above these energies, low reflectivity and finish errors limit efficiency
  - Long focal lengths (> 1 m)

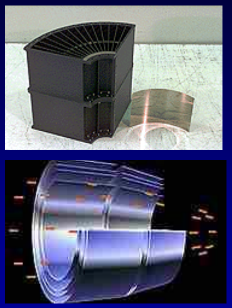

Reflection/Diffraction

P.J. Serlemitsos and Y. Soong,
“Foil x-ray mirrors,” Astrophysics
and Space Science, vol. 239, pp. 177-196, 1996

P.J. Serlemitsos, “Conical Foil X-ray Mirrors:
Performance and Projections,” Applied Optics,
Vol. 27, pg. 1544, 1988

G. Hildebrandt and H. Bradazek
“Approaching Real X-ray Optics,”
The Rigaku Journal, vol. 17(1), pp. 13-22, 2000.

M.J. Pivovaroff, W.C. Barber, F.E. Christensen, W.W. Craig, T. Decker, M. Epstein, T. Funk, C.J. Hailey, B.H. Hasegawa, R. Hill, J.G. Jernigan, C. Taylor, and K. Ziock, “Small Animal Radionuclide Imaging with Focusing Gamma-ray Optics”, Proc. SPIE, Vol. 5199, pp. 147-161, 2004.

M.J. Pivovaroff, T. Funk, W.C. Barber, B.D. Ramsey, B.H. Hasegawa, “Progress of focusing x-ray and gamma-ray optics for small animal imaging”, Proc. SPIE, Vol. 5923, pp. 65-78, 2005.

Absorption

- Imaginary portion of complex index of refraction
- $I(E)/I_0(E) = e^{-\mu(z,E)x}$
- At 140 keV,

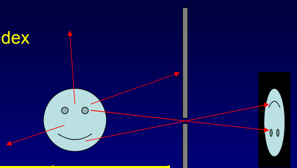

Element	Z	Absorption Coeff (cm^{-1})	Absorption Length (mm)	Transmittance (1/8” material)
H_2O	8	.15	67	95/100
Pb	82	26.823	.373	1/5,000
W	74	36.333	.275	1/100,000
Au	79	42.629	.235	1/1,000,000
Pt	78	43.831	.228	1/1,000,000

Absorption

- Pinholes
- Collimators
- Multi-pinholes & coded apertures

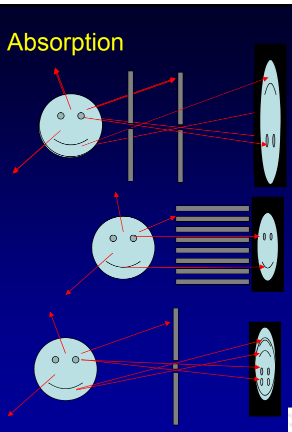

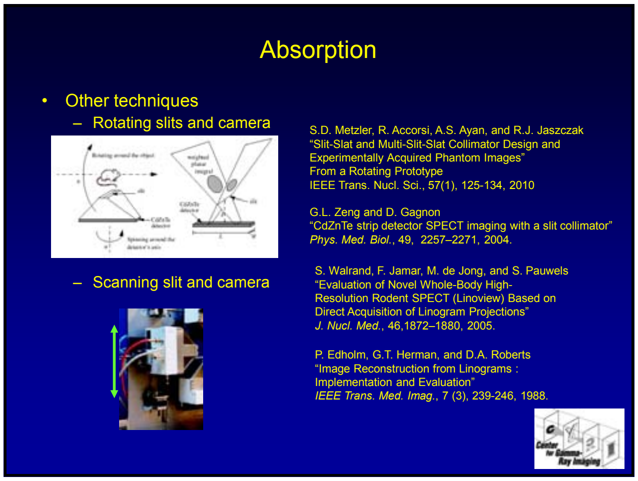

Absorption

- Other techniques
  - Rotating slits and camera
  - Scanning slit and camera

S.D. Metzler, R. Accorsi, A.S. Ayan, and R.J. Jaszczak
"Slit-Slat and Multi-Slit-Slat Collimator Design and
Experimentally Acquired Phantom Images"
From a Rotating Prototype
IEEE Trans. Nucl. Sci., 57(1), 125-134, 2010

G.L. Zeng and D. Gagnon
"CdZnTe strip detector SPECT imaging with a slit collimator"
Phys. Med. Biol., 49, 2257–2271, 2004.

S. Walrand, F. Jamar, M. de Jong, and S. Pauwels
"Evaluation of Novel Whole-Body High-Resolution Rodent SPECT (Linoview) Based on
Direct Acquisition of Linogram Projections"
J. Nucl. Med., 46,1872–1880, 2005.

P. Edholm, G.T. Herman, and D.A. Roberts
"Image Reconstruction from Linograms :
Implementation and Evaluation"
IEEE Trans. Med. Imag., 7 (3), 239-246, 1988.

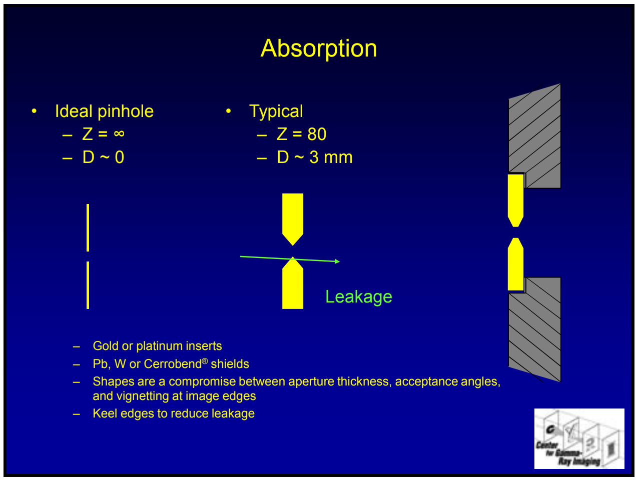

Absorption

- Ideal pinhole
  - Z = ∞
  - D ~ 0
- Typical
  - Z = 80
  - D ~ 3 mm

- Gold or platinum inserts
- Pb, W or Cerrobend® shields
- Shapes are a compromise between aperture thickness, acceptance angles, and vignetting at image edges
- Keel edges to reduce leakage

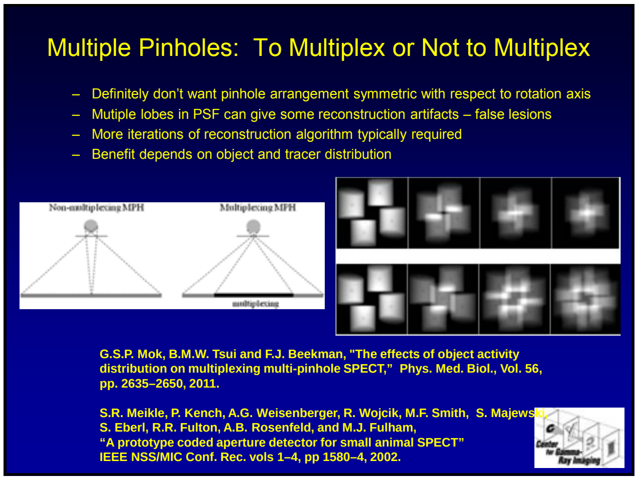

Multiple Pinholes: To Multiplex or Not to Multiplex

- Definitely don't want pinhole arrangement symmetric with respect to rotation axis
- Mutiple lobes in PSF can give some reconstruction artifacts – false lesions
- More iterations of reconstruction algorithm typically required
- Benefit depends on object and tracer distribution

G.S.P. Mok, B.M.W. Tsui and F.J. Beekman, "The effects of object activity distribution on multiplexing multi-pinhole SPECT," Phys. Med. Biol., Vol. 56, pp. 2635–2650, 2011.

**S.R. Meikle, P. Kench, A.G. Weisenberger, R. Wojcik, M.F. Smith, S. Majewski,
S. Eberl, R.R. Fulton, A.B. Rosenfeld, and M.J. Fulham,
"A prototype coded aperture detector for small animal SPECT"
IEEE NSS/MIC Conf. Rec. vols 1–4, pp 1580–4, 2002.**

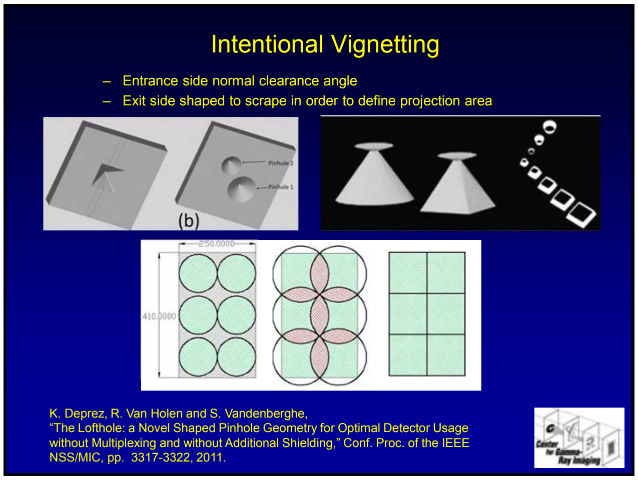

Intentional Vignetting

- Entrance side normal clearance angle
- Exit side shaped to scrape in order to define projection area

K. Deprez, R. Van Holen and S. Vandenberghe,
"The Lofthole: a Novel Shaped Pinhole Geometry for Optimal Detector Usage without Multiplexing and without Additional Shielding," Conf. Proc. of the IEEE NSS/MIC, pp. 3317-3322, 2011.

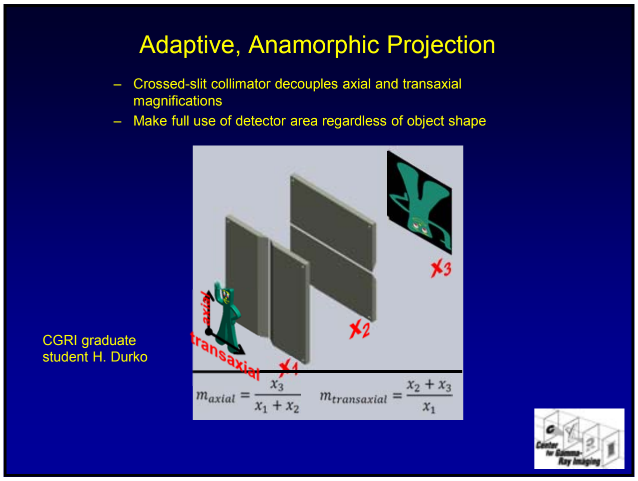

Adaptive, Anamorphic Projection

- Crossed-slit collimator decouples axial and transaxial magnifications
- Make full use of detector area regardless of object shape

$$m_{axial} = \frac{x_3}{x_1 + x_2} \qquad m_{transaxial} = \frac{x_2 + x_3}{x_1}$$

CGRI graduate
student H. Durko

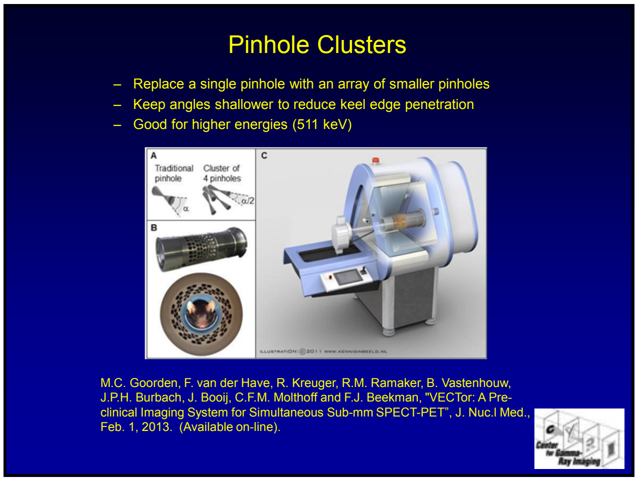

Pinhole Clusters

- Replace a single pinhole with an array of smaller pinholes
- Keep angles shallower to reduce keel edge penetration
- Good for higher energies (511 keV)

M.C. Goorden, F. van der Have, R. Kreuger, R.M. Ramaker, B. Vastenhouw, J.P.H. Burbach, J. Booij, C.F.M. Molthoff and F.J. Beekman, "VECTor: A Pre-clinical Imaging System for Simultaneous Sub-mm SPECT-PET", J. Nuc.l Med., Feb. 1, 2013. (Available on-line).

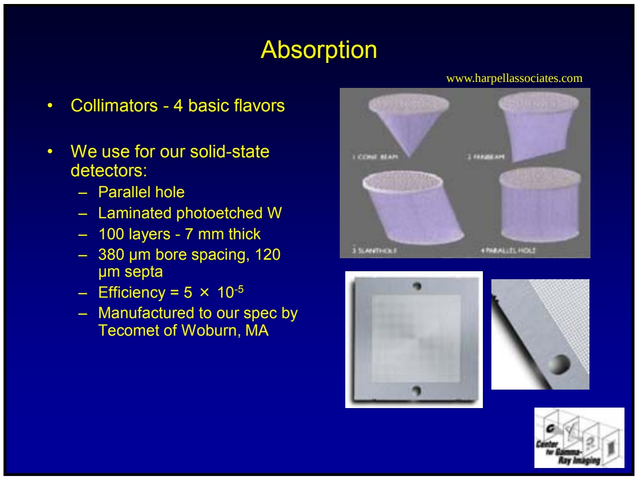

Absorption

www.harpellassociates.com

- Collimators - 4 basic flavors
- We use for our solid-state detectors:
  - Parallel hole
  - Laminated photoetched W
  - 100 layers - 7 mm thick
  - 380 µm bore spacing, 120 µm septa
  - Efficiency = 5 × 10^{-5}
  - Manufactured to our spec by Tecomet of Woburn, MA

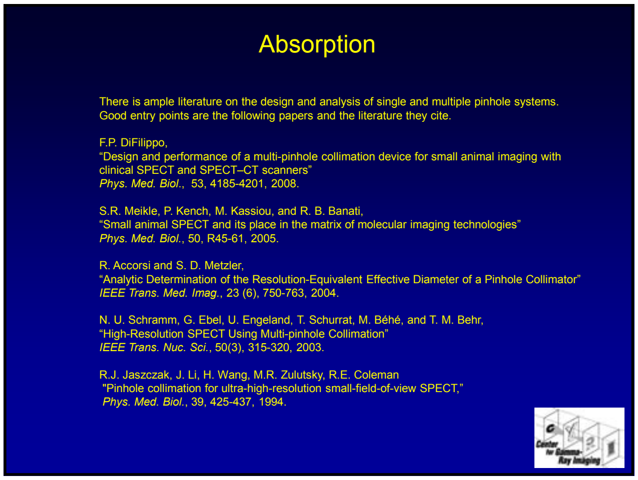

Absorption

There is ample literature on the design and analysis of single and multiple pinhole systems. Good entry points are the following papers and the literature they cite.

F.P. DiFilippo,
“Design and performance of a multi-pinhole collimation device for small animal imaging with clinical SPECT and SPECT–CT scanners”
Phys. Med. Biol., 53, 4185-4201, 2008.

S.R. Meikle, P. Kench, M. Kassiou, and R. B. Banati,
“Small animal SPECT and its place in the matrix of molecular imaging technologies”
Phys. Med. Biol., 50, R45-61, 2005.

R. Accorsi and S. D. Metzler,
“Analytic Determination of the Resolution-Equivalent Effective Diameter of a Pinhole Collimator”
IEEE Trans. Med. Imag., 23 (6), 750-763, 2004.

N. U. Schramm, G. Ebel, U. Engeland, T. Schurrat, M. Béhé, and T. M. Behr,
“High-Resolution SPECT Using Multi-pinhole Collimation”
IEEE Trans. Nuc. Sci., 50(3), 315-320, 2003.

R.J. Jaszczak, J. Li, H. Wang, M.R. Zulutsky, R.E. Coleman
"Pinhole collimation for ultra-high-resolution small-field-of-view SPECT,"
Phys. Med. Biol., 39, 425-437, 1994.

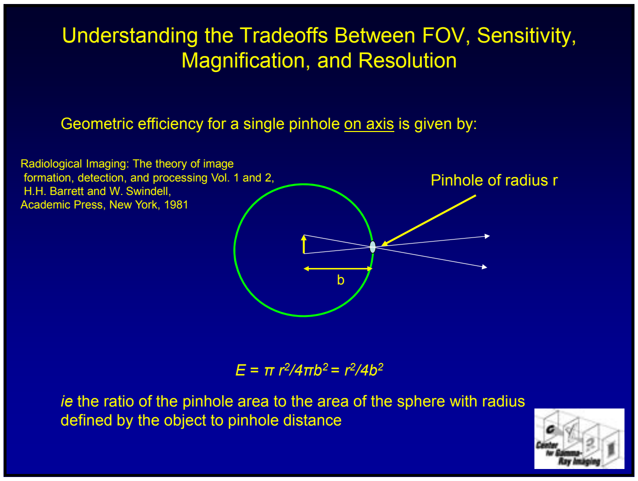

Understanding the Tradeoffs Between FOV, Sensitivity, Magnification, and Resolution

Geometric efficiency for a single pinhole on axis is given by:

Radiological Imaging: The theory of image
formation, detection, and processing Vol. 1 and 2,
H.H. Barrett and W. Swindell,
Academic Press, New York, 1981

$E = \pi r^2/4\pi b^2 = r^2/4b^2$

ie the ratio of the pinhole area to the area of the sphere with radius defined by the object to pinhole distance

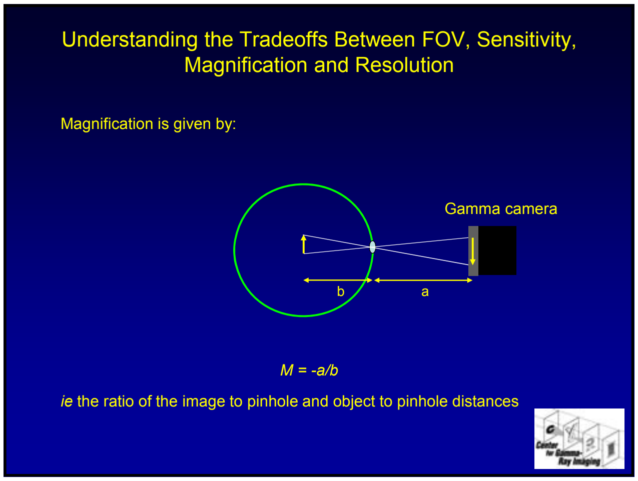

Understanding the Tradeoffs Between FOV, Sensitivity, Magnification and Resolution

Magnification is given by:

$M = -a/b$

ie the ratio of the image to pinhole and object to pinhole distances

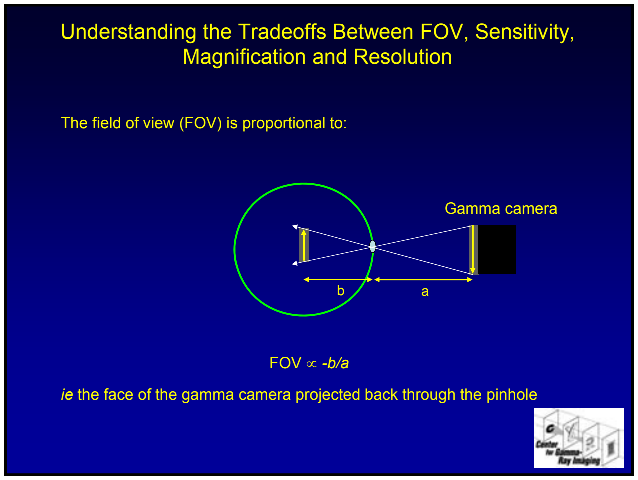

Understanding the Tradeoffs Between FOV, Sensitivity, Magnification and Resolution

The field of view (FOV) is proportional to:

FOV $\propto -b/a$

ie the face of the gamma camera projected back through the pinhole

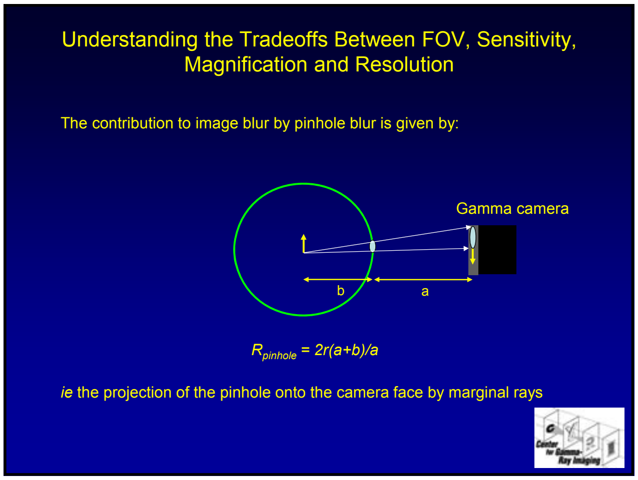

Understanding the Tradeoffs Between FOV, Sensitivity, Magnification and Resolution

The contribution to image blur by pinhole blur is given by:

$R_{pinhole} = 2r(a+b)/a$

ie the projection of the pinhole onto the camera face by marginal rays

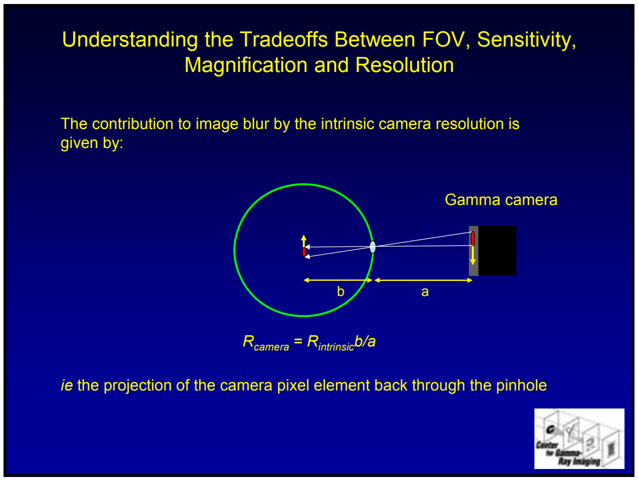

Understanding the Tradeoffs Between FOV, Sensitivity, Magnification and Resolution

The contribution to image blur by the intrinsic camera resolution is given by:

Gamma camera

b

a

$R_{camera} = R_{intrinsic} b/a$

ie the projection of the camera pixel element back through the pinhole

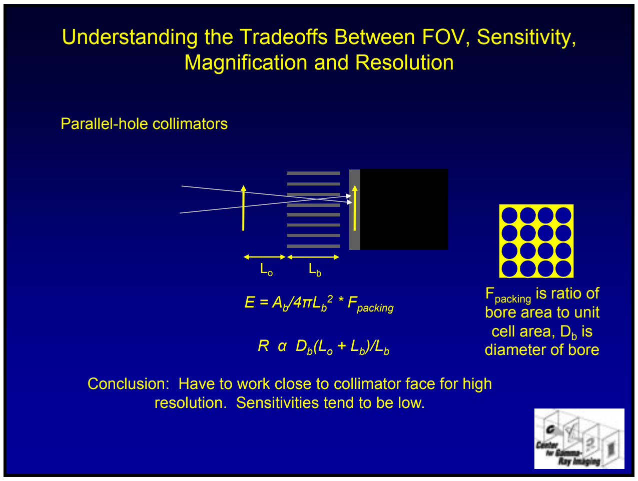

Understanding the Tradeoffs Between FOV, Sensitivity, Magnification and Resolution

Parallel-hole collimators

L_o L_b

$E = A_b/4\pi L_b^2 * F_{packing}$

$R \;\alpha\; D_b(L_o + L_b)/L_b$

$F_{packing}$ is ratio of bore area to unit cell area, D_b is diameter of bore

Conclusion: Have to work close to collimator face for high resolution. Sensitivities tend to be low.

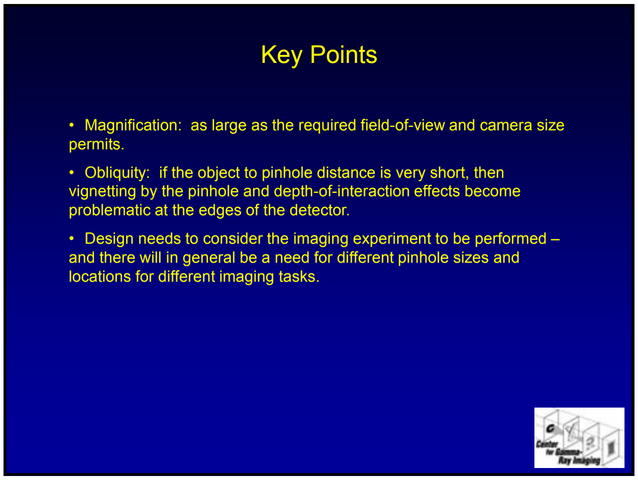

Key Points

- Magnification: as large as the required field-of-view and camera size permits.
- Obliquity: if the object to pinhole distance is very short, then vignetting by the pinhole and depth-of-interaction effects become problematic at the edges of the detector.
- Design needs to consider the imaging experiment to be performed – and there will in general be a need for different pinhole sizes and locations for different imaging tasks.

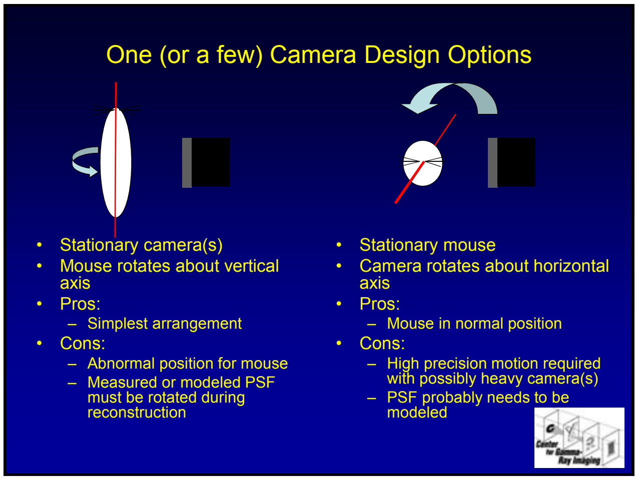

One (or a few) Camera Design Options

- Stationary camera(s)
- Mouse rotates about vertical axis
- Pros:
  - Simplest arrangement
- Cons:
  - Abnormal position for mouse
  - Measured or modeled PSF must be rotated during reconstruction

- Stationary mouse
- Camera rotates about horizontal axis
- Pros:
  - Mouse in normal position
- Cons:
  - High precision motion required with possibly heavy camera(s)
  - PSF probably needs to be modeled

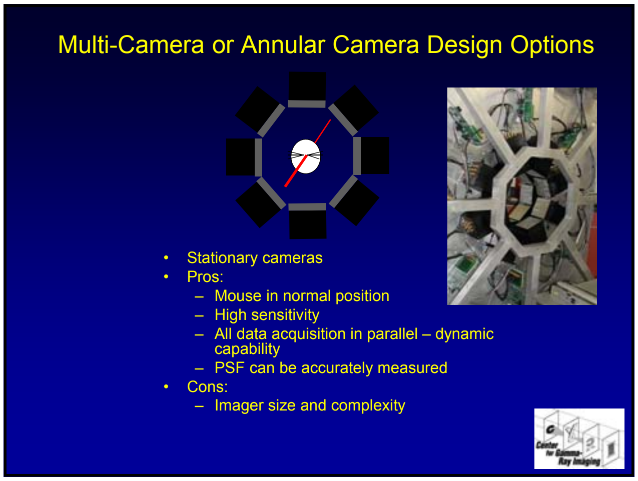

Multi-Camera or Annular Camera Design Options

- Stationary cameras
- Pros:
  - Mouse in normal position
  - High sensitivity
  - All data acquisition in parallel – dynamic capability
  - PSF can be accurately measured
- Cons:
  - Imager size and complexity

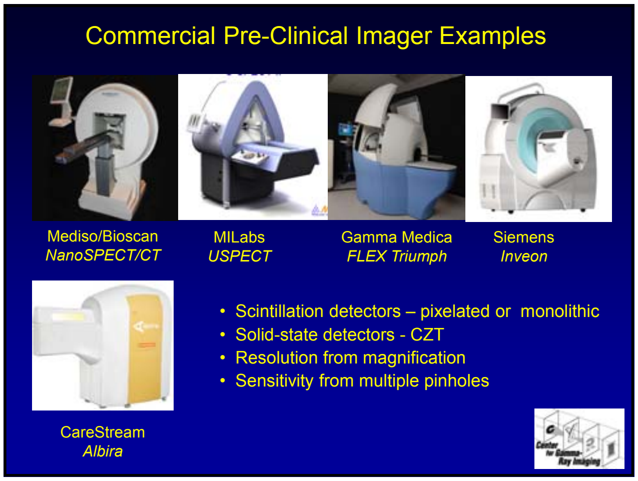

Commercial Pre-Clinical Imager Examples

Mediso/Bioscan *NanoSPECT/CT*

MILabs *USPECT*

Gamma Medica *FLEX Triumph*

Siemens *Inveon*

CareStream *Albira*

- Scintillation detectors – pixelated or monolithic
- Solid-state detectors - CZT
- Resolution from magnification
- Sensitivity from multiple pinholes

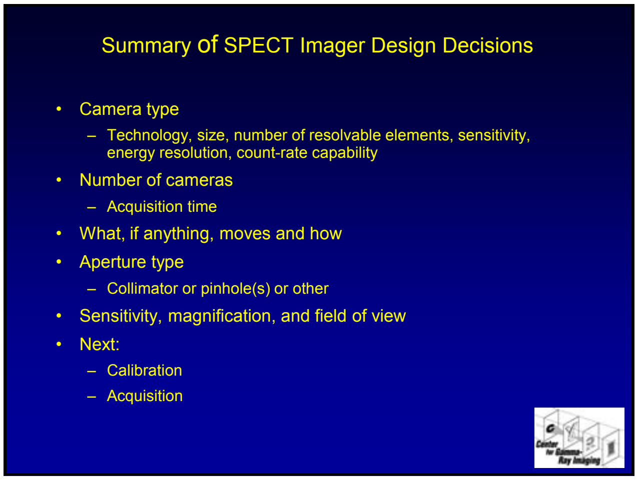

Summary of SPECT Imager Design Decisions

- Camera type
  - Technology, size, number of resolvable elements, sensitivity, energy resolution, count-rate capability
- Number of cameras
  - Acquisition time
- What, if anything, moves and how
- Aperture type
  - Collimator or pinhole(s) or other
- Sensitivity, magnification, and field of view
- Next:
  - Calibration
  - Acquisition

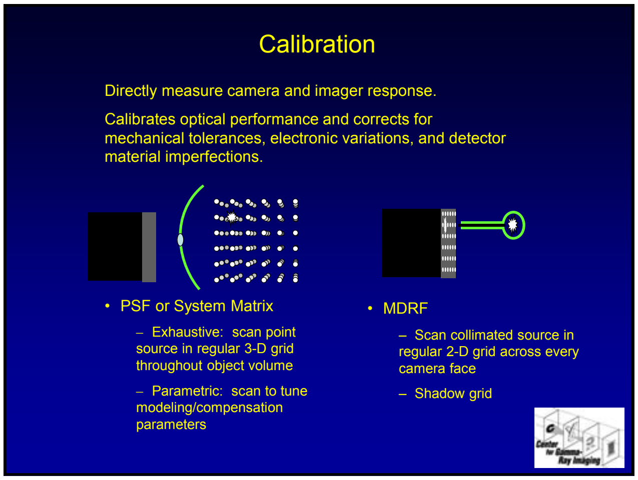

Calibration

Directly measure camera and imager response.

Calibrates optical performance and corrects for mechanical tolerances, electronic variations, and detector material imperfections.

- PSF or System Matrix
  - Exhaustive: scan point source in regular 3-D grid throughout object volume
  - Parametric: scan to tune modeling/compensation parameters
- MDRF
  - Scan collimated source in regular 2-D grid across every camera face
  - Shadow grid

Calibration Stages

Rotation and secondary translation makes it easy to scan the source precisely above each camera face.

Mean Detector Response Function (MDRF) Calibration

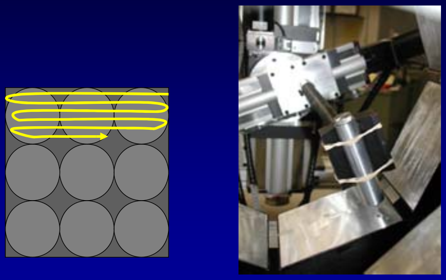

Calibration References

F. van der Have, B. Vastenhouw, M. Rentmeester, and F.J. Beekman
“System Calibration and Statistical Image Reconstruction for Ultra-High Resolution Stationary Pinhole SPECT”
IEEE Trans. Med. Imag., 27(7), 960-971, 2008

Y-C. Chen, L.R. Furenlid, D.W. Wilson, and H.H. Barrett,
“Calibration of Scintillation Cameras and Pinhole SPECT Imaging Systems”
Chap. 12 in Small-Animal SPECT Imaging. New York: Springer Science Business Media, 195–201, 2005.

And references therein.

Trends

- Data processing and acquisition benefit from the rapid pace of technology development in:
  - Fast, low-noise op amps and A/D converters
  - Readout ASICS
  - GPUs and FPGAs
  - Networking and communications
  - Computing power and storage capacities

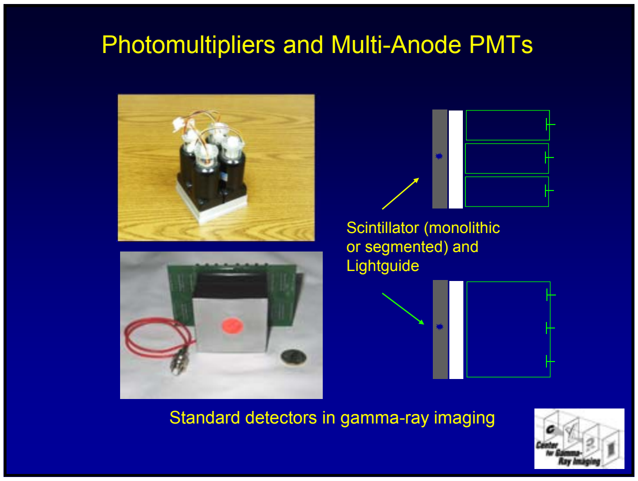

Photomultipliers and Multi-Anode PMTs

Scintillator (monolithic or segmented) and Lightguide

Standard detectors in gamma-ray imaging

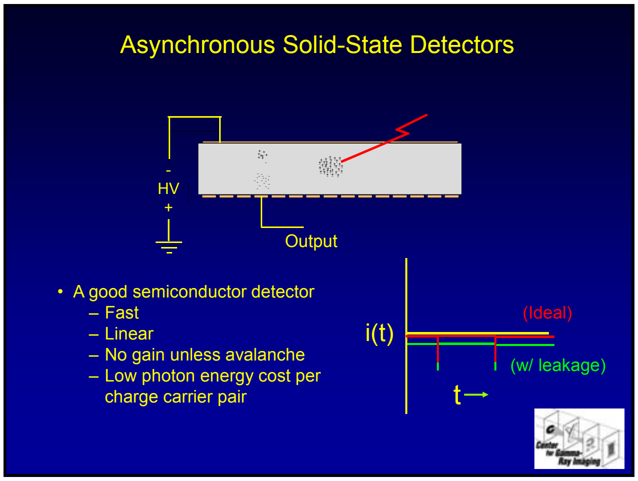

Asynchronous Solid-State Detectors

- A good semiconductor detector
  - Fast
  - Linear
  - No gain unless avalanche
  - Low photon energy cost per charge carrier pair

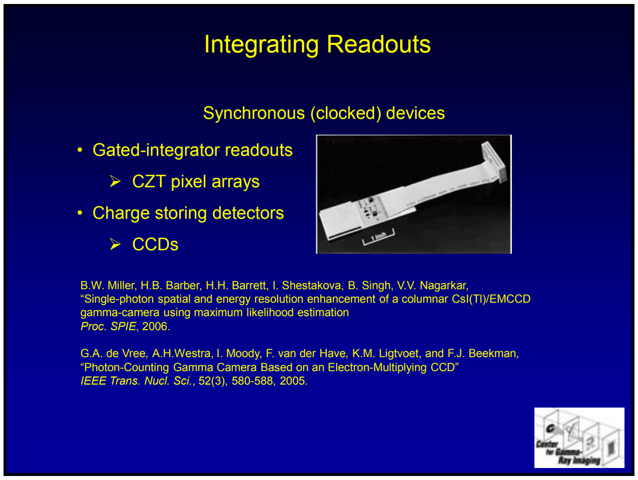

Integrating Readouts

Synchronous (clocked) devices

- Gated-integrator readouts
  - CZT pixel arrays
- Charge storing detectors
  - CCDs

B.W. Miller, H.B. Barber, H.H. Barrett, I. Shestakova, B. Singh, V.V. Nagarkar, "Single-photon spatial and energy resolution enhancement of a columnar CsI(Tl)/EMCCD gamma-camera using maximum likelihood estimation *Proc. SPIE*, 2006.

G.A. de Vree, A.H.Westra, I. Moody, F. van der Have, K.M. Ligtvoet, and F.J. Beekman, "Photon-Counting Gamma Camera Based on an Electron-Multiplying CCD" *IEEE Trans. Nucl. Sci.*, 52(3), 580-588, 2005.

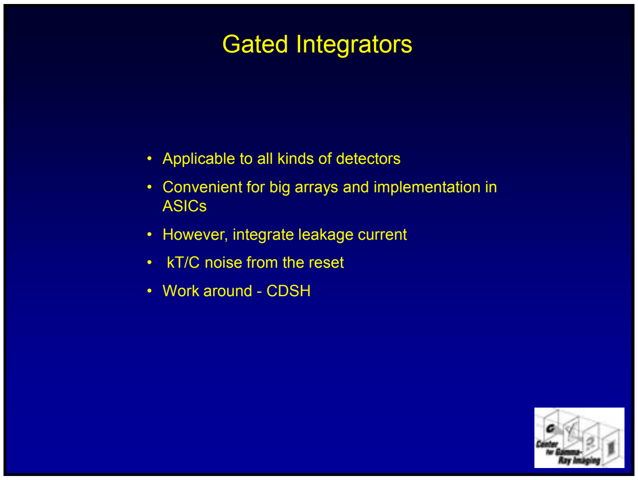

Gated Integrators

- Applicable to all kinds of detectors
- Convenient for big arrays and implementation in ASICs
- However, integrate leakage current
- kT/C noise from the reset
- Work around - CDSH

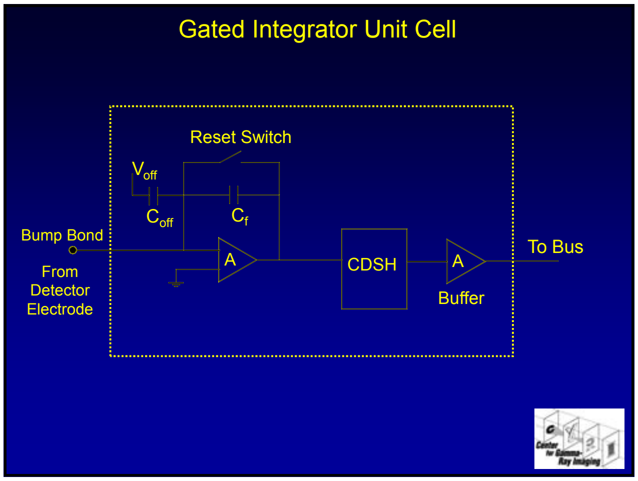

Gated Integrator Unit Cell

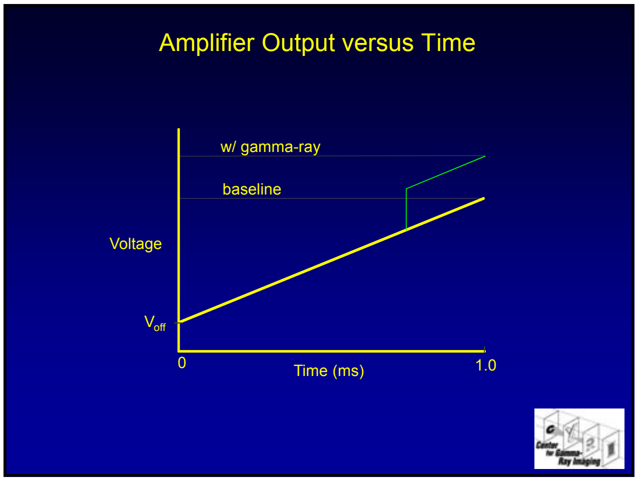

Amplifier Output versus Time

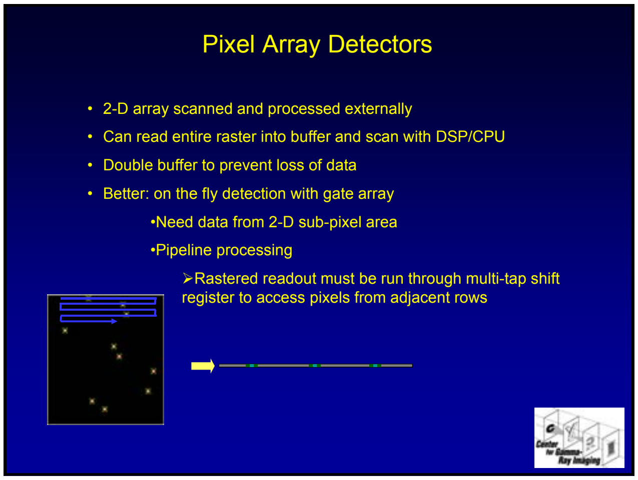

Pixel Array Detectors

- 2-D array scanned and processed externally
- Can read entire raster into buffer and scan with DSP/CPU
- Double buffer to prevent loss of data
- Better: on the fly detection with gate array
  - •Need data from 2-D sub-pixel area
  - •Pipeline processing
    - ➢Rastered readout must be run through multi-tap shift register to access pixels from adjacent rows

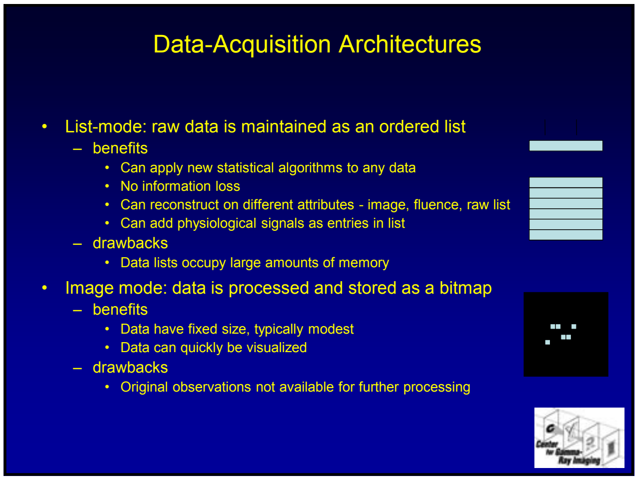

Data-Acquisition Architectures

- List-mode: raw data is maintained as an ordered list
  - benefits
    - Can apply new statistical algorithms to any data
    - No information loss
    - Can reconstruct on different attributes - image, fluence, raw list
    - Can add physiological signals as entries in list
  - drawbacks
    - Data lists occupy large amounts of memory
- Image mode: data is processed and stored as a bitmap
  - benefits
    - Data have fixed size, typically modest
    - Data can quickly be visualized
  - drawbacks
    - Original observations not available for further processing

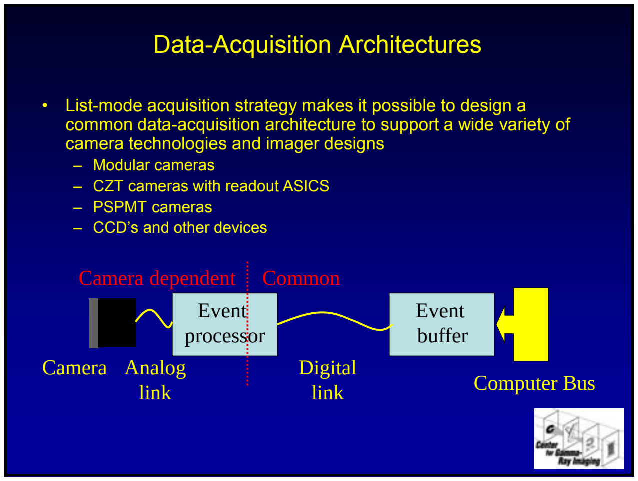

Data-Acquisition Architectures

- List-mode acquisition strategy makes it possible to design a common data-acquisition architecture to support a wide variety of camera technologies and imager designs
  - Modular cameras
  - CZT cameras with readout ASICS
  - PSPMT cameras
  - CCD's and other devices

Camera dependent
Common
Camera
Analog link
Event processor
Digital link
Event buffer
Computer Bus

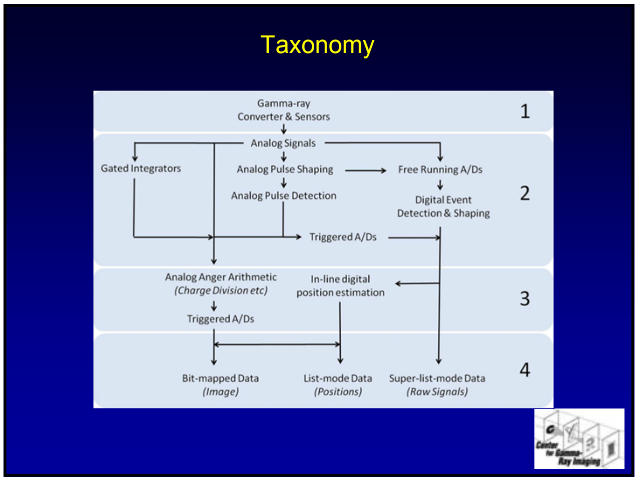

Taxonomy

1
Gamma-ray Converter & Sensors

2
Analog Signals
Gated Integrators
Analog Pulse Shaping
Free Running A/Ds
Analog Pulse Detection
Digital Event Detection & Shaping
Triggered A/Ds

3
Analog Anger Arithmetic *(Charge Division etc)*
Triggered A/Ds
In-line digital position estimation

4
Bit-mapped Data *(Image)*
List-mode Data *(Positions)*
Super-list-mode Data *(Raw Signals)*

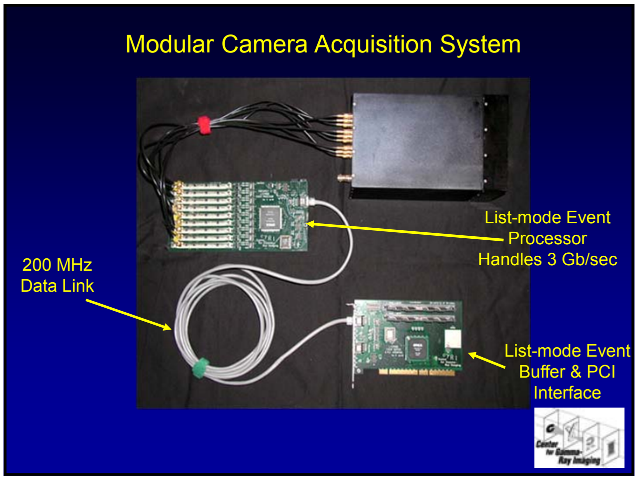

Modular Camera Acquisition System

200 MHz Data Link
List-mode Event Processor Handles 3 Gb/sec
List-mode Event Buffer & PCI Interface

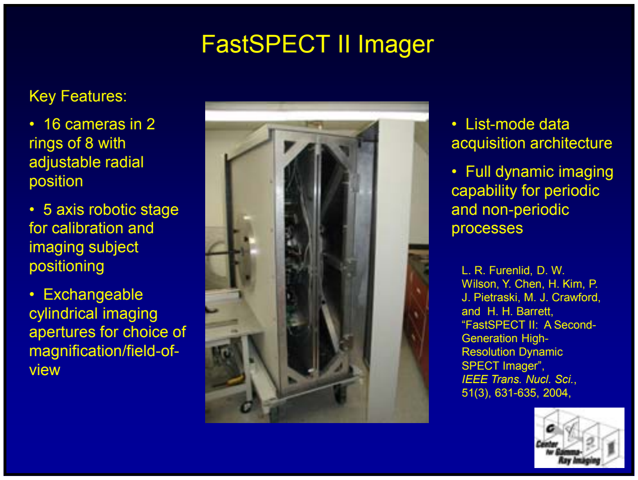

FastSPECT II Imager

Key Features:

- 16 cameras in 2 rings of 8 with adjustable radial position
- 5 axis robotic stage for calibration and imaging subject positioning
- Exchangeable cylindrical imaging apertures for choice of magnification/field-of-view

- List-mode data acquisition architecture
- Full dynamic imaging capability for periodic and non-periodic processes

L. R. Furenlid, D. W. Wilson, Y. Chen, H. Kim, P. J. Pietraski, M. J. Crawford, and H. H. Barrett, "FastSPECT II: A Second-Generation High-Resolution Dynamic SPECT Imager", *IEEE Trans. Nucl. Sci.*, 51(3), 631-635, 2004,

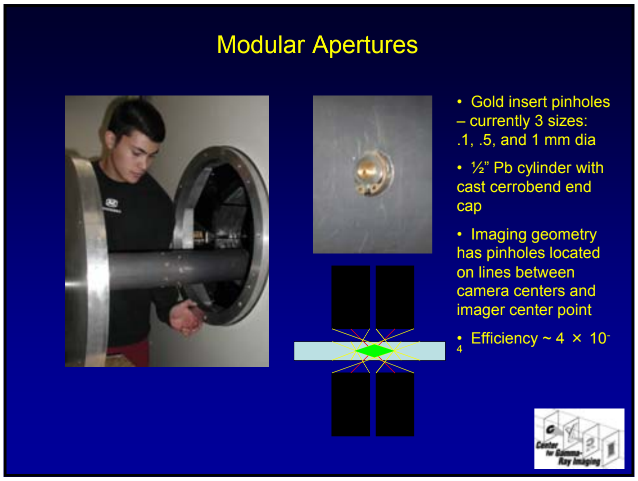

Modular Apertures

- Gold insert pinholes – currently 3 sizes: .1, .5, and 1 mm dia
- ½” Pb cylinder with cast cerrobend end cap
- Imaging geometry has pinholes located on lines between camera centers and imager center point
- Efficiency ~ 4 × 10^{-4}

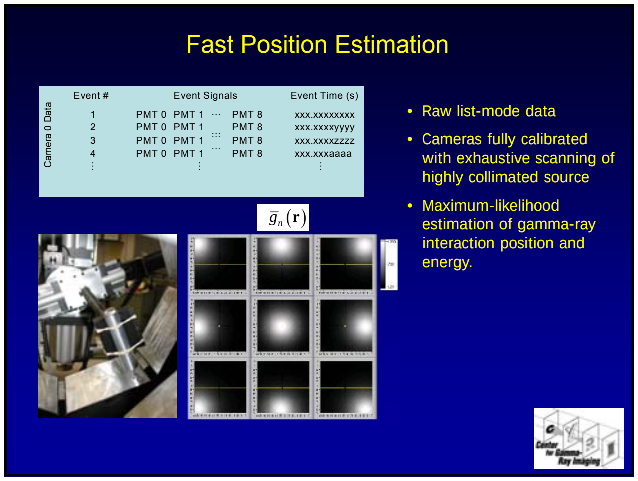

Fast Position Estimation

Camera 0 Data

Event #	Event Signals				Event Time (s)
1	PMT 0	PMT 1	⋯	PMT 8	xxx.xxxxxxxx
2	PMT 0	PMT 1		PMT 8	xxx.xxxxyyyy
3	PMT 0	PMT 1	⋮	PMT 8	xxx.xxxxzzzz
4	PMT 0	PMT 1	⋯	PMT 8	xxx.xxxaaaa
⋮		⋮			⋮

$\bar{g}_n(\mathbf{r})$

- Raw list-mode data
- Cameras fully calibrated with exhaustive scanning of highly collimated source
- Maximum-likelihood estimation of gamma-ray interaction position and energy.

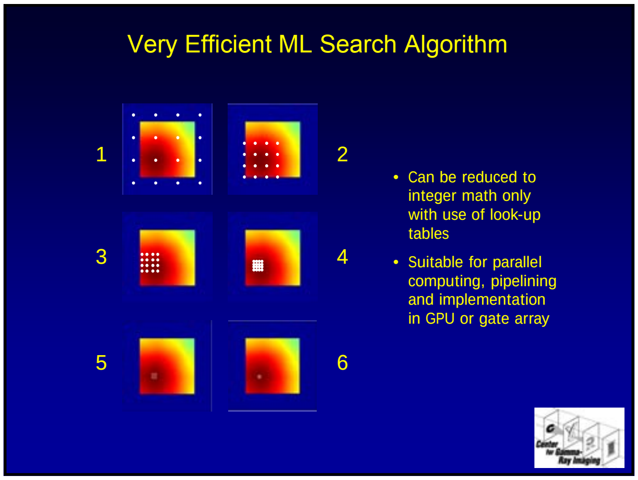

Very Efficient ML Search Algorithm

- Can be reduced to integer math only with use of look-up tables
- Suitable for parallel computing, pipelining and implementation in GPU or gate array

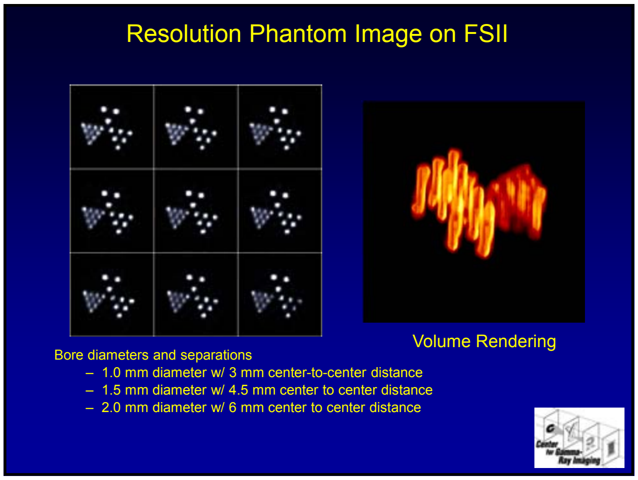

Resolution Phantom Image on FSII

Volume Rendering

Bore diameters and separations
- 1.0 mm diameter w/ 3 mm center-to-center distance
- 1.5 mm diameter w/ 4.5 mm center to center distance
- 2.0 mm diameter w/ 6 mm center to center distance

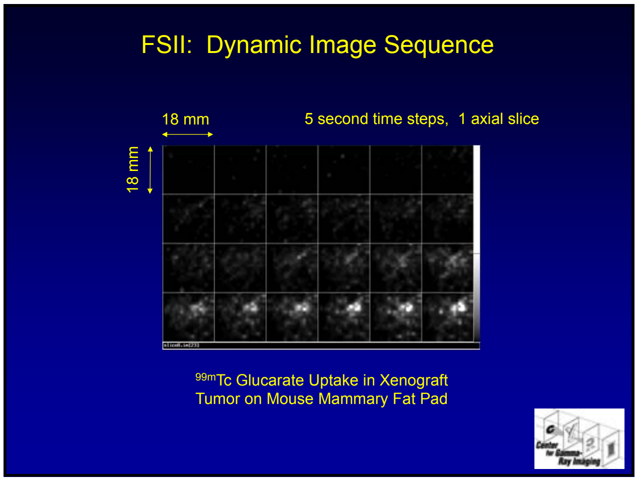

FSII: Dynamic Image Sequence

18 mm

5 second time steps, 1 axial slice

18 mm

^{99m}Tc Glucarate Uptake in Xenograft
Tumor on Mouse Mammary Fat Pad

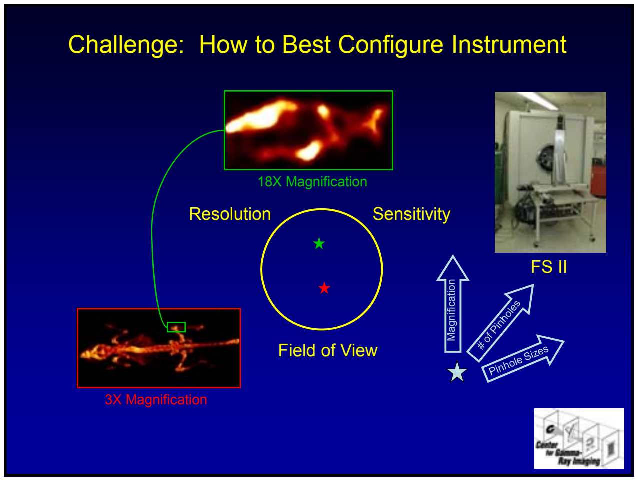

Challenge: How to Best Configure Instrument

18X Magnification

Resolution

Sensitivity

Field of View

3X Magnification

FS II

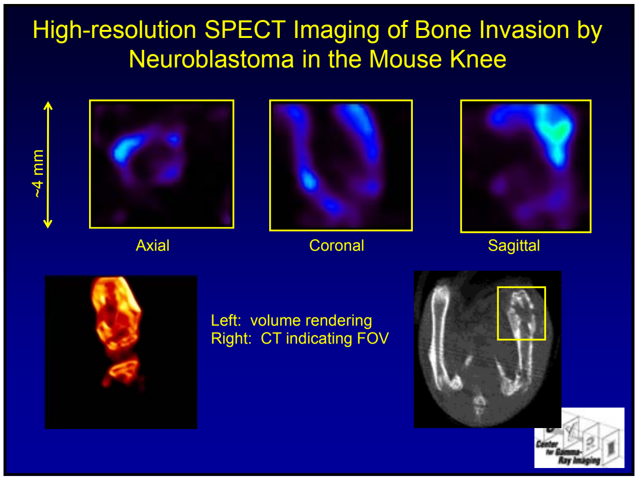

High-resolution SPECT Imaging of Bone Invasion by Neuroblastoma in the Mouse Knee

~4 mm

Axial

Coronal

Sagittal

Left: volume rendering
Right: CT indicating FOV

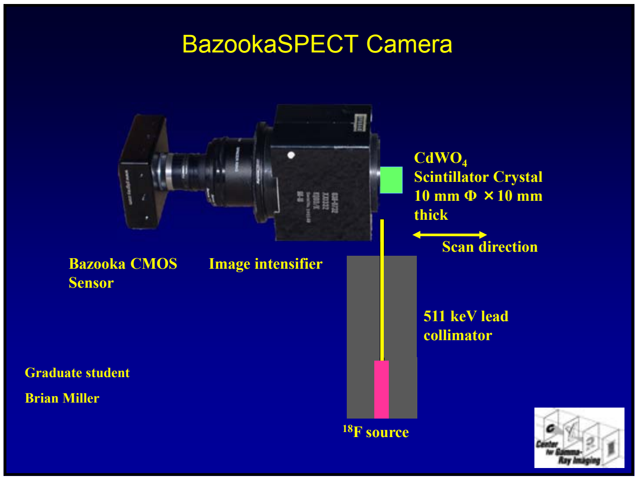

BazookaSPECT Camera

CdWO$_4$ Scintillator Crystal 10 mm Φ × 10 mm thick

Scan direction

Bazooka CMOS Sensor

Image intensifier

511 keV lead collimator

Graduate student

Brian Miller

^{18}F source

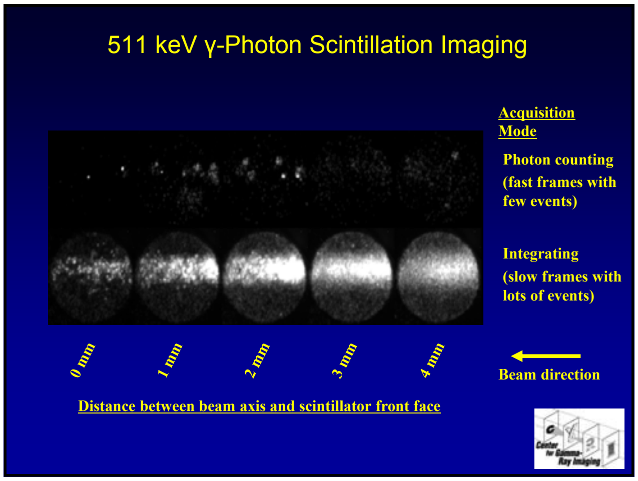

511 keV γ-Photon Scintillation Imaging

Acquisition Mode

Photon counting (fast frames with few events)

Integrating (slow frames with lots of events)

← Beam direction

Distance between beam axis and scintillator front face

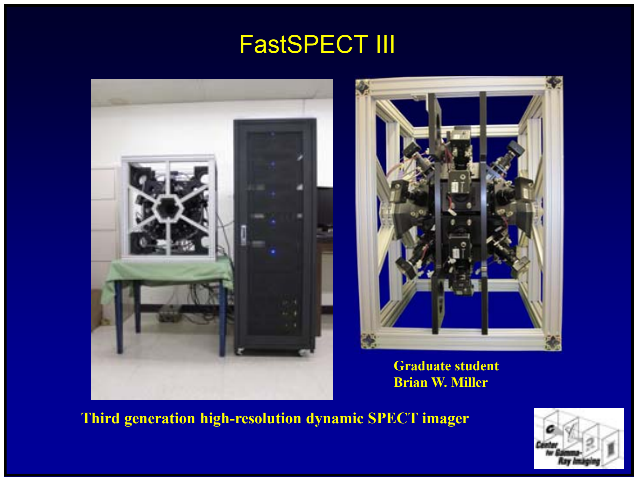

FastSPECT III

Graduate student Brian W. Miller

Third generation high-resolution dynamic SPECT imager

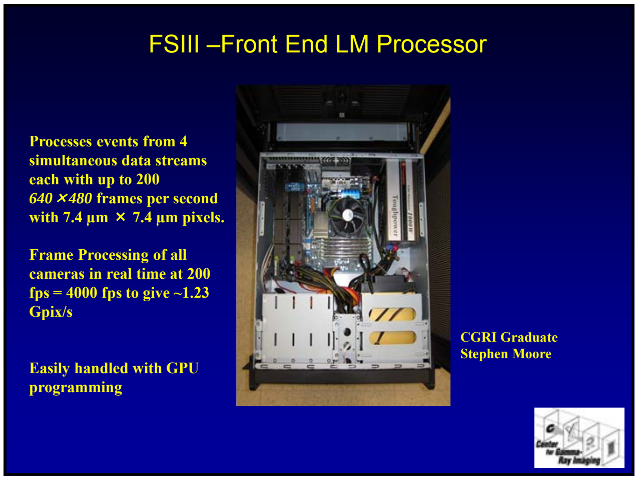

FSIII –Front End LM Processor

Processes events from 4 simultaneous data streams each with up to 200 *640 ×480* frames per second with 7.4 µm × 7.4 µm pixels.

Frame Processing of all cameras in real time at 200 fps = 4000 fps to give ~1.23 Gpix/s

Easily handled with GPU programming

CGRI Graduate Stephen Moore

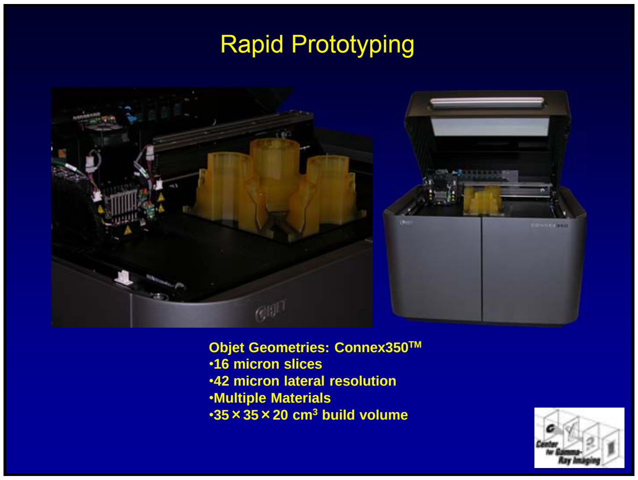

Rapid Prototyping

Objet Geometries: Connex350™
- **16 micron slices**
- **42 micron lateral resolution**
- **Multiple Materials**
- **35 × 35 × 20 cm³ build volume**

FastSPECT III Imaging Aperture

Casting:
W powder/epoxy resin

Pt metal

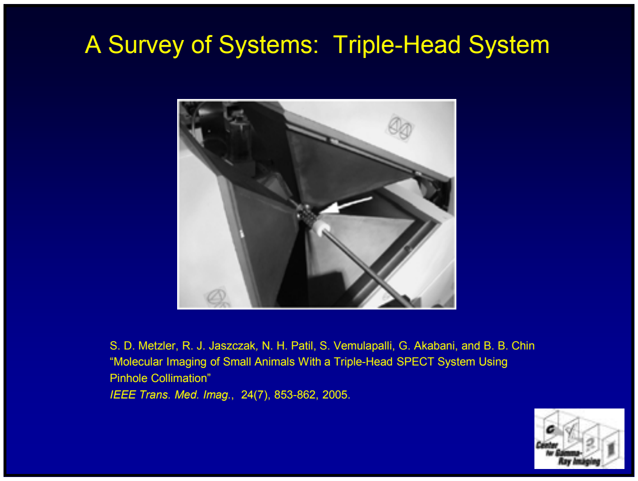

A Survey of Systems: Triple-Head System

S. D. Metzler, R. J. Jaszczak, N. H. Patil, S. Vemulapalli, G. Akabani, and B. B. Chin
"Molecular Imaging of Small Animals With a Triple-Head SPECT System Using Pinhole Collimation"
IEEE Trans. Med. Imag., 24(7), 853-862, 2005.

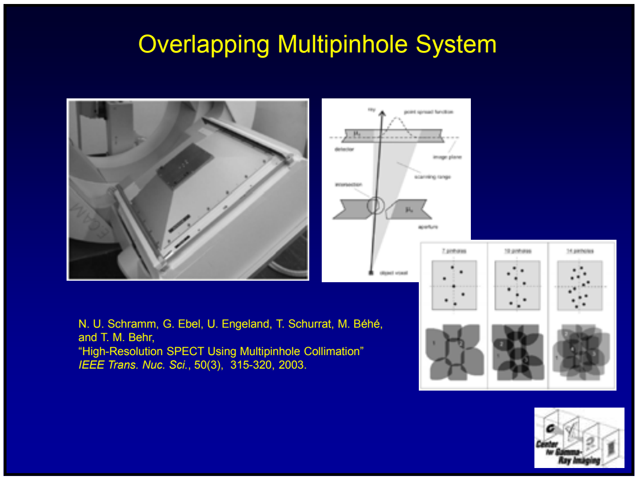

Overlapping Multipinhole System

N. U. Schramm, G. Ebel, U. Engeland, T. Schurrat, M. Béhé, and T. M. Behr,
"High-Resolution SPECT Using Multipinhole Collimation"
IEEE Trans. Nuc. Sci., 50(3), 315-320, 2003.

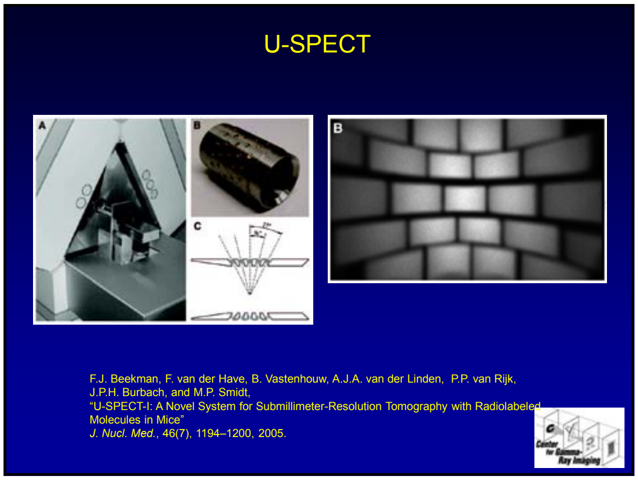

U-SPECT

F.J. Beekman, F. van der Have, B. Vastenhouw, A.J.A. van der Linden, P.P. van Rijk, J.P.H. Burbach, and M.P. Smidt,
"U-SPECT-I: A Novel System for Submillimeter-Resolution Tomography with Radiolabeled Molecules in Mice"
J. Nucl. Med., 46(7), 1194–1200, 2005.

U-SPECT/CT

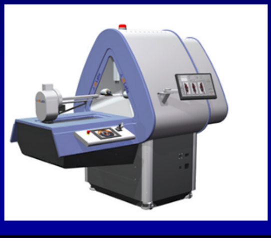

SPECT-CT

Courtesy of
MILabs

New Line of SPECT/PET-MRs

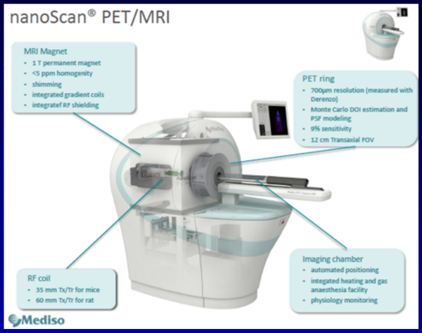

nanoScan® PET/MRI

MRI Magnet
- 1 T permanent magnet
- <5 ppm homogenity
- shimming
- integrated gradient coils
- integratef RF shielding

PET ring
- 700µm resolution (measured with Derenzo)
- Monte Carlo DOI estimation and PSF modeling
- 9% sensitivity
- 12 cm Transaxial FOV

RF coil
- 35 mm Tx/Tr for mice
- 60 mm Tx/Tr for rat

Imaging chamber
- automated positioning
- integated heating and gas anaesthesia facility
- physiology monitoring

Non-overlapping Projections

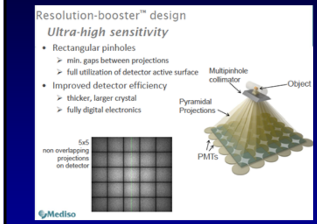

Resolution-booster™ design

Ultra-high sensitivity

- Rectangular pinholes
  - min. gaps between projections
  - full utilization of detector active surface
- Improved detector efficiency
  - thicker, larger crystal
  - fully digital electronics

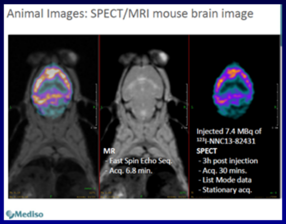

Animal Images: SPECT/MRI mouse brain image

MR
- Fast Spin Echo Seq.
- Acq. 6.8 min.

Injected 7.4 MBq of ^{123}I-NNC13-82431

SPECT
- 3h post injection
- Acq. 30 mins.
- List Mode data
- Stationary acq.

Superposition of MR soft-tissue and SPECT images

Conclusions

- On-going rapid developments: imaging principles, detectors, systems and computing resources (GPUs)
- List-mode architectures have advantages, including ability to support new camera technologies without having to reinvent software and data links
- Careful calibration critical for optimal system performance
- Stationary imager designs permit dynamic and high-throughput studies
- System design process can/should be thoroughly guided by simulations with realistic digital phantoms.

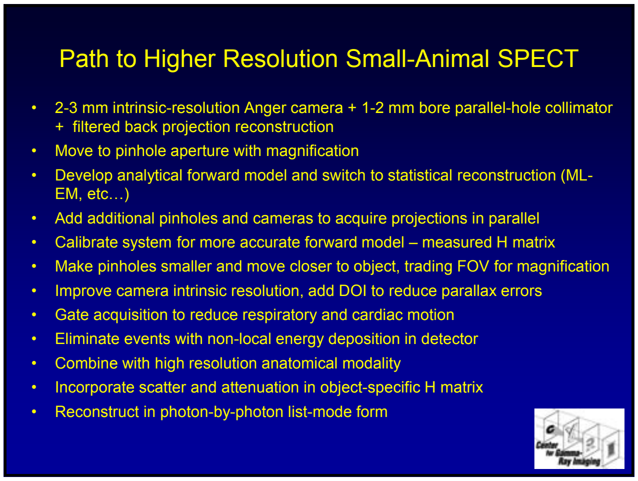

Path to Higher Resolution Small-Animal SPECT

- 2-3 mm intrinsic-resolution Anger camera + 1-2 mm bore parallel-hole collimator + filtered back projection reconstruction
- Move to pinhole aperture with magnification
- Develop analytical forward model and switch to statistical reconstruction (ML-EM, etc…)
- Add additional pinholes and cameras to acquire projections in parallel
- Calibrate system for more accurate forward model – measured H matrix
- Make pinholes smaller and move closer to object, trading FOV for magnification
- Improve camera intrinsic resolution, add DOI to reduce parallax errors
- Gate acquisition to reduce respiratory and cardiac motion
- Eliminate events with non-local energy deposition in detector
- Combine with high resolution anatomical modality
- Incorporate scatter and attenuation in object-specific H matrix
- Reconstruct in photon-by-photon list-mode form